Ecosystems (2024) 27: 493–507
https://doi.org/10.1007/s10021-024-00901-4

Bioturbation by Benthic Stingrays Alters the Biogeomorphology of Tidal Flats

Janne Nauta,[1,2]* Guido Leurs,[1,3] Brian O. Nieuwenhuis,[1,8] Donné R. A. H. Mathijssen,[1,9] Han Olff,[1] Tjeerd J. Bouma,[1,4,5,6] Daphnevan der Wal,[4,7] Nadia Hijner,[1] Aissa Regalla,[10] Samuel Ledo Pontes,[10] and Laura L. Govers[1,3]

[1]*Conservation Ecology Group, Groningen Institute for Evolutionary Life Sciences, University of Groningen, 9700 CC Groningen, The Netherlands;* [2]*Forest and Nature Conservation, Van Hall Larenstein, University of Applied Sciences, Velp, The Netherlands;* [3]*Department Coastal Systems, Royal Netherlands Institute of Sea Research, Utrecht University, 1790 AB Den Burg, The Netherlands;* [4]*Department of Estuarine and Delta Systems, Royal Netherlands Institute of Sea Research, Utrecht University, 4401 NT Yerseke, The Netherlands;* [5]*Department of Physical Geography, Faculty of Geosciences, Utrecht University, 3508 TC Utrecht, The Netherlands;* [6]*Delta Academy Applied Research Centre, HZ University of Applied Sciences, Postbus 364, 4380 AJ Vlissingen, The Netherlands;* [7]*Faculty of Geo-Information Science and Earth Observation (ITC), University of Twente, P.O. Box 217, 7500 AE Enschede, The Netherlands;* [8]*Red Sea Research Center, King Abdullah University of Science and Technology, 23955-6900 Thuwal, Saudi Arabia;* [9]*Aquaculture and Fisheries Group (AFI), Wageningen University, 6708 WD Wageningen, The Netherlands;* [10]*Institute of Biodiversity and Protected Areas (IBAP), Bissau, Guinea-Bissau*

Abstract

Fishing-down-marine-food-webs has resulted in alarming declines of various species worldwide. Benthic rays are one examples of such overexploited species. On tidal flats, these rays are highly abundant and play an ecologically important role. They use tidal flats as refuge, feeding and resting grounds, during which they bury into the sediment, which results in sediment bioturbation. Changes in bioturbation intensity, following ray removal, may affect the biogeomorphology of tidal flats with possible cascading effects on the macrozoobenthic community. However, it is poorly understood how these indirect effects could influence ecosystem function. We therefore studied the geomorphic impact of benthic rays (specifically the pearl whipray/stingray *Fontitrygon margaritella*) on the tropical tidal flats of the Bijagós Archipelago, Guinea-Bissau, on a landscape scale. We investigated 1) bioturbation rates by rays using drone and ground surveys, 2) the spatial distribution of ray pits on multiple tidal flats, 3) the impact of rays on sediment properties and macrozoobenthos by experimental exclusion (15 months). Benthic rays bioturbated 3.7 ± 0.35% of the tidal flat's sediment surface per day over one single 24-h period, which equals a complete top-sediment-surface turnover every 27 days. The spatial distribution of ray pits was affected by tidal flat geomorphology since pits decayed faster at areas exposed to strong hydrodynamic forces. Predator exclusion altered sedi-

Received 17 May 2023; accepted 2 January 2024;
published online 20 February 2024

Supplementary Information: The online version contains supplementary material available at https://doi.org/10.1007/s10021-024-00901-4.

Author contributions JN: writing - original draft, conceptualization, methodology, formal analysis,investigation, visualization, supervision. GL: writing - review and editing,conceptualization, investigation. BON: writing - review and editing, formalanalysis, investigation. DRAHM: writing - review and editing, formalanalysis, investigation. HO: writing - review and editing, conceptualization, projectadministration, funding acquisition. TJB: writing - review and editing,conceptualization. DW: writing - review and editing, conceptualization.NH: writing - review and editing, investigation. AR: resources. SLP: resources. LLG: writing - review and editing, conceptualization,investigation, supervision, project administration, funding acquisition.

**Corresponding author; e-mail:* janne.nauta@gmail.com

ment properties, leading to changes in sedimentation (− 17%) and erosion (− 43%) rates. In addition, macrozoobenthic species composition changed, marked by an increase in Capitellidae worms and a greater biomass of Malacostraca over time. These changes indicated substantial effects of ray bioturbation on the biotic and geomorphic landscape of tidal flats. Overall, we conclude that changing abundances of benthic rays can have clear landscape-wide geomorphological effects on intertidal ecosystems. These indirect consequences of fisheries should be incorporated in integrative management plans to preserve tidal flats and connected ecosystems.

Key words: bioturbation; ray pits; biogeomorphology; stingrays; tidal flats; ray overexploitation; the pearl whipray.

Introduction

Tidal flats are prominent and productive geomorphic systems that provide valuable ecosystem services such as carbon storage, nutrient fluxes, coastal defense, primary and secondary productivity, fisheries enhancement and connection between marine and terrestrial ecosystems (Temmerman and others 2013; Alongi 2014, 2018; van de Koppel and others 2015; van der Zee and others 2016). However, 16% of the world's tidal flats have been lost due to anthropogenic pressures between 1984 and 2016 (Murray and others 2019). Anthropogenic stressors, such as fishing, may disrupt natural equilibria with potential consequences for associated fauna and the ecological interaction networks they are part of Pinnegar and others (2000). Knowledge gaps on the interaction between threats (for example, coastal fisheries), ecological functioning (for example, food web structure, community composition) and the geomorphological development of tidal flats (for example, sedimentation, elevation) need to be addressed to improve effective management of these ecologically important areas because global losses of tidal areas are still ongoing (Hill and others 2021; Murray and others 2022).

Fishing activities have caused dramatic declines in Chondrichthyes—shark, ray and chimera populations on a global scale (Stevens and others 2000; Baum and others 2003; Baum and Myers 2004; Sherman and others 2023), leading to an estimated 32% of 1199 species currently being threatened with extinction (Dulvy and others 2021). Although shark and ray species that use tidal habitats are mostly affected by coastal mixed-species fisheries, they are also affected by industrial fisheries that operate on the edges of tidal waters to catch animals that migrate into subtidal offshore areas (Dulvy and others 2014; Leurs and others 2021).

Most elasmobranchs are characterized by large body sizes, slow growth rates, late maturity, low fecundity and consequently highly vulnerable to both direct human exploitation and bycatch mortality (Winemiller and Rose 1992; Jennings and others 2001). Larger individuals are predicted to feed at higher trophic levels because size determines the dimensions of prey sizes that a predator can consume (Cohen and others 1993). Larger predator overexploitation can control prey abundance through top-down processes (Bascompte and others 2005), causing an increase in prey abundance (Myers and others 2007; Ferretti and others 2010; Sherman and others 2020). But, these predator–prey dynamics need further investigation (Grubbs and others 2016). On the other hand, when species of larger body size decline, fishing pressure may shift to smaller elasmobranchs such as benthic rays, known as 'fishing down the food web' (Pauly 1998). However, knowledge on the consequences of reduced ray numbers on ecosystem functioning is limited (Flowers and others 2021).

Bioturbating benthic rays actively alter their habitats (that is, habitat-modifiers) in search for food or resting grounds. To do so, these rays excavate and rework the sediment (hereafter referred to as 'ray pits') through a combination of protrusion of the jaws, water-jetting through the spiracles and by flapping their pectoral fins (Freitas and others 2019; Figure 1). These bioturbating activities can alter the sediment erodibility and composition (Takeuchi and Tamaki 2014) and create physical microhabitats that can be beneficial to other species. For instance, ray pits can collect high amounts of organic matter which benefits benthic detritus feeders (O'Shea and others 2012). Bioturbation by rays thus alters geomorphological and ecological processes which may ultimately affect ecosystem functioning of tidal flats (Lynn-Myrick and Flessa 1996; Needham and others 2011; O'Shea and others 2012). Moreover, these rays can be highly abundant in tidal ecosystems and therefore play an ecologically important role (Leurs and others 2023a).

While the local-scale bioturbating effects of benthic rays are well studied (Grant 1983; O'Shea and others 2012; Myrick and Flessa 2017), approaches to upscale these processes to a landscape scale are limited. In addition, experimental ap-

proaches to support ray bioturbation effects are inadequate (O'Shea 2012; Flowers and others 2021). We therefore studied the geomorphological impact of benthic rays using the tropical tidal flats of the Bijagós Archipelago, Guinea-Bissau. Specifically, we quantified 1) the extent and intensity of benthic ray bioturbation at the tidal flat landscape scale by conducting ground and drone surveys, 2) the spatial distribution and longevity of ray pits by looking at ray pit densities throughout the archipelago to test if the abundance of ray pits could be influenced by tidal flat morphology (for example, ray pits erode faster under highly hydrodynamic conditions Shea and others 2012) and 3) the effect of ray bioturbation on sediment properties and macrozoobenthos by means of a ray exclusion experiment. The study area was chosen to investigate the effects of benthic ray feeding behavior since tidal flats are key-habitats for benthic rays (Leurs and others 2023a). In the Bijagós Archipelago, 896–2685 rays were captured daily if, respectively, 30% and 100% of the fishing fleet was active in 2020 (Leurs and others unpublished). This is likely an underestimation of the actual catch as vessels from neighboring countries were unaccounted for (Leurs and others unpublished). As global (including West African) coastal fisheries are currently increasing with an alarming rate (Dulvy and others 2021; Leurs and others 2021), studying the geomorphic effects of bioturbating rays right now is relevant because changes in population densities of these fishery-targeted species may affect their ecosystem and conservation status of benthic rays continues to deteriorate (Sherman and others 2023).

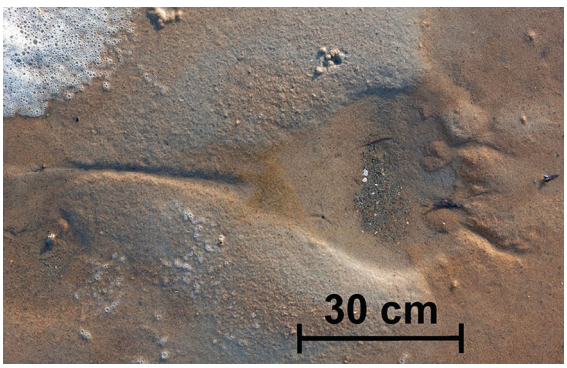

Figure 1. Excavation of the sediment created by benthic rays, called a ray pit.

Methods

Study Site

The Bijagós Archipelagos, west coast of Guinea-Bissau, supports extensive protected tidal flat areas where fisheries are restricted (Diop and Dossa 2011; Hill and others 2021). These areas provide refuge for globally threatened elasmobranchs, including benthic rays (Diop and Dossa 2011; Campredon and Catry 2016). Therefore, this area is highly suitable for studying the landscape-scale effects of these habitat modifying species. *Fontitrygon margaritella* is the most common species that could make ray pits as observed on the tidal flats (Leurs and others 2023a, b). However, ruling out *Fontitrygon margarita* completely is impossible only from pit formations. We also know that the large majority (140 out of 143, 97.9%) of *Fontitrygon* spp. sampled in the archipelago were *F. margaritella* from fish market sampling for stomach contents (Clements and others 2022). These results combined give a solid indication that the large majority of pits are created by *F. margaritella*. The archipelago islands consist of 88 islands and islets, which are the remaining peaks of the eroded and flooded sedimentary basin of the ancient delta of the Rio Grande and Rio Geba, off the coast of West Africa (Bird 2011) surrounded by mangroves and 760 km^2 of tidal flats (Meijer and others 2021). These islands are located at the most southern end of the Senegalo-Mauritanian sedimentary basin, and sediments originate mostly from the Corubal en Geba rivers (Campredon and Catry 2016). These sediments are deposited and transported by complex hydrodynamic forces in a network of river channels. On the other hand, high annual rainfall (2200 mm) leads to high surface erosion rates (Bird 2011). The temperate southern Africa realm has a relative stable tidal wetland (tidal flats, tidal marsh and mangrove ecosystems) coastline (Murray and others 2022). The Bijagós archipelago has the highest tidal range of the West African coast with spring tides reaching up to 4.5 m amplitude with strong currents up to 78 cm/s (Campredon and Catry 2016). These tidal flats support approximately 700,000 waders along the East-Atlantic Flyway (Salvig and others 1994; Van Roomen and others 2011; Campredon and Catry 2016), and because of the archipelago's extraordinary biodiversity, it has been classified as a 'UNESCO Biosphere Reserve' in 1996 and as a 'Ramsar site' in 2014 (Ramsar Convention Secretariat 2014). Our research in the Bijagós Archipelagos took place

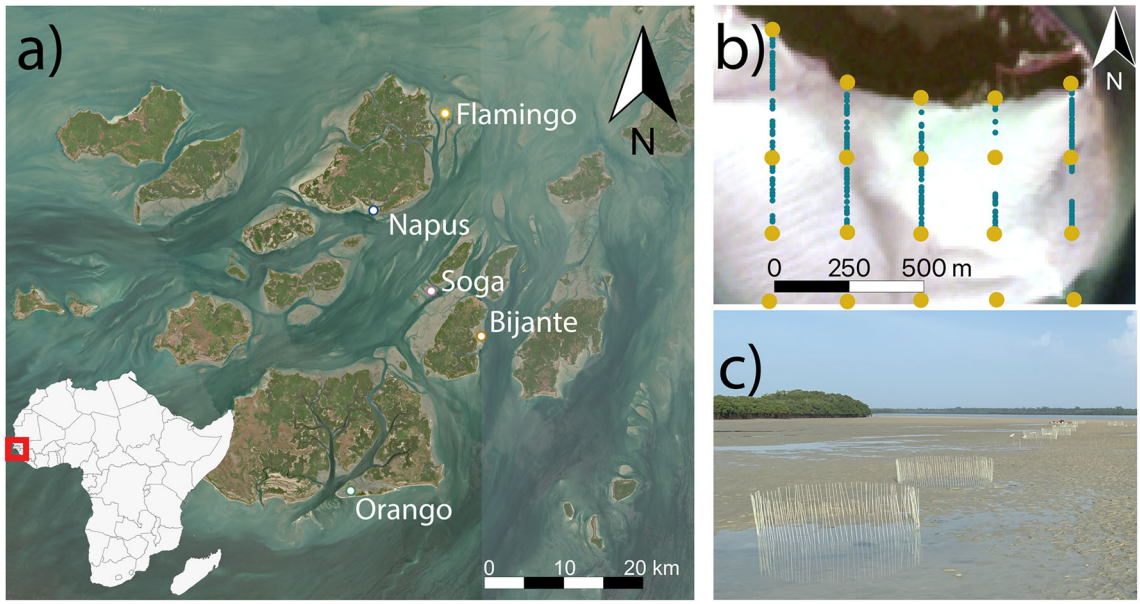

Figure 2. Overview of the study area on the west coast of Guinea-Bissau, West Africa (bottom left), zoomed in on red square (Sentinel-2 L2A, resolution: 10 m, True color, 0% cloud cover, date: 2019/03/16): **a** the tidal flats named Napus, Orango, Bijante, Flamingo and Soga in the Bijagós Archipelago; **b** an example of the observational survey at Napus through transects (250 m between each transect) perpendicular to the mangrove fringe towards the subtidal area, where dots indicate ray pit abundances (blue) and sample locations of macrozoobenthos cores (yellow); **c** picture of the predator exclosure experimental setup.

during the period of October–December 2019 and February 2021 (Figure 2a).

Quantifying the Extent of Benthic Ray Bioturbation—Drone Survey

We mapped benthic-ray bioturbation pits of the Napus mudflat with a DJI Mavic 2 Pro drone (RGB) on February 15 and 16, 2021. For this, the high-resolution images (ground resolution = 0.5 cm/pixel) taken by the drone were stitched together using PIX4D. The mapped area covered an L-shape section of ~ 4.6 hectares, where the L-shape area was chosen to cover as much tidal flats heterogeneity (for example, sediment type and bathymetric elevation) as possible within the drone battery supply for 1 day. This image was overlaid with 64 squares of 16 m^2 each and positioned to capture as much spatial variation in ray pit abundance as possible. In every square, ray pits were manually annotated by visual observations in QGIS (QGIS Development Team and others 2018; version 3.6.3). To identify ray pits from other excavations (formed by other organisms or footprints), we color-marked all observed excavations in the field and consequently detected the differences in the size and shape of the excavations on drone images. Other organisms (than stingrays) that may bioturbate the sediments of the Bijagós Archipelago are cownose rays, fiddler crabs and calianassid shrimps (Suchanek and Colin 1986; El-Hacen and others 2019; Flowers and others 2021). We identified the ray pits in this study from other excavations based on the size and shape of the pits that relates to the disk width of the ray which is around 34 cm for stingrays (Figure 1; Leurs and others unpublished). Cownose ray pits (disk width up to 1 m (Smith and Merriner 1985) are bigger than stingrays (Leurs and others 2023a), and fiddler crabs and calianassid shrimps create smaller excavations (Suchanek and Colin 1986). For each of these squares, we compared the image of February 15 to that of February 16 and counted all newly formed ray pits. We analyzed the distribution of the newly formed ray pits according normal (linear models; LM) and concentrated distribution (generalized linear models with Poisson or negative binomial distribution) and compared the Akaike information criterions for small sample size (AICs). To translate ray pit surface coverage into bioturbation rates, we used the amount of newly formed pits and the average pit volume measured in November 2019 (see first two Results sections).

We performed all statistical analyses in R (R Core Team 2017; version 4.0.3): a language for statistical computing and graphics. We validated all model

assumptions by plotting 1) residuals versus fitted values to verify homogeneity, 2) QQ-plots of the residuals to test for normality and 3) residuals versus each explanatory variable to check for independence. In addition, Shapiro–Wilks's test ($p > 0.05$) and Bartlett's test ($p > 0.05$) were used to test for normality and homogeneity of variance, respectively. Surface bioturbated per day was log transformed to meet model assumptions and analyzed by LM. Post hoc comparisons were used to test for significant differences between the five tidal flats (r-package 'emmeans'; (Lenth 2019)). The relationship between pit counts on February 15 and 16 was fitted to a linear regression model.

Landscape-Scale Spatial Ray Pit Distribution—Observation Surveys Across the Region

We quantified ray pit occurrence through transects counts (Figure 2b) for five sites across the archipelago (Bijante = Bijante, Bubaque, N11° 15′ 24.3″ W15° 50′ 09.6″; Flamingo = Banco de Flamingo, Maio, Urok, N11° 33′ 18.1″ W15° 53′ 14.3″; Orango = Adonge, Orangozinho, N11° 02′ 10.2″ W16° 00′ 58.0″; Napus = Napus, Formosa, Urok, N11° 25′ 33.1″ W15° 58′ 59.3″; and Soga = Encromas, N11° 18′ 47.1″ W15° 54′ 01.1″). At each location, we sampled transects ($n = 5$ per location, but Soga $n = 4$, with 250 m distance between the transects) that covered the entire morphologic landscape of the tidal flat and that was accessible by foot (from the edge of the subtidal to the mangrove edge). Along each transect, all ray pits that were within 1 m of the transect line were measured. Of each ray pit the length diameter, width diameter, depth radius and water depth were measured. Additionally, the location of each ray pit was measured at 1 cm precision with a RTK dGPS (Trimble R8, GNSS-receiver) connected to a local base station as a reference point. Small benthic rays in the Bijagós Archipelago are mostly represented by the most common occurring stingray species, the pearl stingray (dominantly *Fontitrygon margaritella*; (Leurs and others 2023b)). Hence, pit volume was calculated by treating the pits as a semi-ellipsoidal shape based on the body shape of the pearl stingray using Eq. 1 (O'Shea 2012; O'Shea and others 2012; Myrick and Flessa 2017):

$$\text{pit volume} = (4/3\pi(L_r * W_r * D_r))/2$$

in which L_r is the length radius (diameter/2), W_r is the width radius (diameter/2), and D_r is the depth radius.

The surface area covered with ray pits of the transects was log transformed and consequently analyzed by LM and Tukey's post hoc comparisons to test for significant differences between the five tidal flats (r-package 'emmeans'; Lenth 2019).

Because of the spatial heterogeneity of the tidal flats, we related the ray pit abundances to environmental parameters. To do so, we measured and/or obtained the parameters of the mudflat characteristics, macrozoobenthos, sediment properties and emergence time. First, we defined mudflats characteristics (that is, distance to mangrove forests, gullies and subtidal waters) through QGIS based on the habitat classification of (Meijer and others 2021), that is, mangrove, mudflat and water depth. Habitat characteristics were manually verified by comparing the habitat classification of Meijer and others (2021) to the satellite images (Sentinel-2 L2A, resolution: 10 m, True color, 0% cloud cover, date: 2019/03/16) and adjusted if needed. For instances, based on field observations, gullies that were known to remain inundated during low tide were added to the gully map. Second, to look at possible food sources of the rays, macrozoobenthos were sampled in a grid of 250 m spread across each tidal flat (Figure 2b, $n = 20$ per tidal flat) with a PVC corer of Ø 15 cm to a depth of ~ 25 cm. Each sample was sieved over a 1 mm round mesh (Compton and others 2013). After sample collection, all macrozoobenthos was fixated in 10% formaldehyde and identified to species level in the laboratory. After identification, species were dried for 24 h at 60 °C and incinerated for 4 h at 550 °C to determine Ash Free Dry Weight (AFDW). Third, sediment samples were taken in the same 250 m grid as the macrozoobenthos samples. To analyze sediment composition, we sampled the top-1 and top-5 cm of the sediment surface with a small core of Ø 2.5 cm and determined organic matter content of the soil, median grainsize D50 (μm) and silt% (grain size < 63 μm). For calculation of organic matter content, AFDW of sediment samples was determined and the percentage weight loss on ignition (LOI $_{wt}$%) was calculated. To measure median grain size and silt%, sediment samples were freeze dried (− 550 C, 48 h), sieved over 1-mm mesh and analyzed with the Malvern Mastersizer 2000 (Malvern Instruments, Worcestershire, UK, serial number 34403/139, model APA 2000 with Hydro G 2000 introduction unit and Autosampler 2000). Last, emergence time was derived from the results of Granadeiro and others (2021) that estimated exposure with Sentinel-2 satellite imagery.

To correlate the environmental parameters to the ray pit abundances, we performed ordinary kriging to interpolate any missing data points for median grainsize D50, silt% and macrozoobenthos AFDW based on the 250 m grid samples (n = 20 samples per tidal flat with a sampling and interpolation coverage of 0.5–0.75 km^2; r-package: 'automap'; Hiemstra, 2022) in R (R Core Team 2020, version 4.0.3). The function 'autoKrige' fits a variogram model to the given data set and returns the results of the interpolation: prediction, variance and standard deviation. The environmental parameters of ray pit abundance were modeled with a generalized additive model (GAM) with smooth splines to allow fitting any nonlinear pattern (r-package 'mgcv'; Wood 2017), where tidal flats were modeled as a random factor. Ray pit abundance was zero-inflated, tested with r-package 'DHARMa'; (Hartig 2023). We tested if the smooth terms were necessary by running the model with and without smooth terms for each predictor separately. The lowest AIC was reached by including smooth terms on all the predictor, except sediment median grain size D50, and significance of smoothers was tested via an adapted Wald test (Wood 2017). The GAM's smoothers were estimated through restricted maximum likelihood to prevent overfitting. Residual spatial autocorrelation was inspected by fitting a GAM with a tensor product of the coordinates to the residuals of the original GAM (Wood 2017). GAM model selection was performed by ranking all possible subsets of the full GAM based on AICc (r-package 'MuMin'; (Bartón 2022)). The optimal subset approach was used because it performs best when comparing models that contain correlating measurements. Adjusted R-squared values were used to assess overall model performance.

To test for the sensitivity of the ray pits longevity to exposure, we measured the longevity of artificial pits (n = 20, starting pit size was 25 × 24 × 4 [L × W × D]) on two locations with expected high and low exposure to hydrodynamic forces. High exposure locations were situated exposed to the incoming tide at 100–300 m to the subtidal waters, whereas low exposure locations were situated at the mangrove edge, sheltered by the tidal flat at 300–500 m to the subtidal waters. Measurements were taken for 84 h with a 12–36 h interval depending on accessibility.

Although we expected differences in exposure to hydrodynamic forces, the locations were chosen based on a comparable elevation, with on average a relative difference of + 8.9 cm at the mangrove edge compared to the exposed location, measured at 1-cm precision with a RTK dGPS (Trimble R8, GNSS-receiver) connected to local base station as a reference point. Ray pit longevity was analyzed with linear regression models.

Ray Bioturbation Effects on Sediment and Macrozoobenthos—Exclusion Experiment

To test the consequences of benthic ray absence on sediment properties and macrozoobenthos, we experimentally excluded predators (for example, rays and birds) with a 15-month exclosure experiment. We installed 30 circular (diameter of 2 m) experimental plots in October 2019 (Figure 2c). We deployed the following experiment treatments: *i)* predator exclosure (exclosure, n = 12), *ii)* effect of exclosure (one sided, open exclosure; n = 6) and *iii)* no exclusion (control; n = 12). Predators were excluded with barriers made of glass-fiber sticks (1 × 0.003 m, length × diameter) inserted halfway (50 cm) into the sediment at a 5 cm interval. For the open exclosure, we constructed plots with only half of the circle (Ø 2 m) covered by glass-fiber sticks to test for geomorphic effects of the exclosure method on sediment properties. These open exclosures were installed with the opening to each of the cardinal directions (n = 3 per cardinal direction, north, east, south and west; total n = 12). The plots were spaced 3.5 m apart in a randomized block design. The contours of the control plots were marked by four sticks which had no further exclosure function. After counting ray pits in the experimental plots, we could confirm that the exclosures were effective for benthic rays since 0 ± 0% (mean ± SE) of the exclosures contained ray pits, compared to 48 ± 6% and 33 ± 6% (mean ± SE) in the open exclosures and control, respectively (Appendix S2). However, the exclosures also seemed to be effective in excluding wading birds since we observed bird foot prints in 5 ± 0% of the exclosures, compared to 42 ± 6% and 45 ± 6% in the open exclosure and control. For the entire duration of the experiment, plots were inspected and maintained for fouling, scouring and missing sticks on average once every 2 months. After 15 months of deployment of the exclosures, we sampled macrozoobenthos and sediment properties. The macrozoobenthos were sampled with a PVC corer of Ø 15 cm to a depth of ~ 25 cm, sieved over a 1 mm round mesh (Compton and others 2013), fixated in 10% formaldehyde and identified to species level in the laboratory. After identification, we measured species abundance and biomass. Species were dried for 24 h at 60 °C and incinerated for 4 h at 550 °C to

determine Ash Free Dry Weight (AFDW). Sediment properties were sampled with a small core of Ø 2.5 cm (the top-1 and top-5 cm of the sediment surface) and analyzed for organic matter content of the soil, median grainsize D50 (µm) and silt% (grain size < 63 µm). To calculate organic matter content (percentage weight loss on ignition (LOI $_{wt}$%)), sediment samples were dried for 24 h at 60 °C and incinerated for 4 h at 550 °C. To measure median grain size and silt%, sediment samples were freeze dried (− 550 °C, 48 h), sieved over 1-mm mesh and analyzed with the Malvern Mastersizer 2000 (Malvern Instruments, Worcestershire, UK, serial number 34403/139, model APA 2000 with Hydro G 2000 introduction unit and Autosampler 2000). In addition, the effect of ray exclusion on sediment dynamics was investigated with sediment erosion pins (Nolte and others 2013). Upon installation in 2019, each plot was equipped with two sediment pins that consisted of a thin one-meter-long metal rod anchored ~ 85 cm into the sediment, with a loosely fitting metal ring surrounding it at the sediment surface. This allowed us to track maximum erosion, sediment accretion and net change of the sediment's surface elevation over the experimental period of 15 months.

The impact of predatory exclusion on macrozoobenthos was visualized using Non-Metric Multidimensional Scaling (NMDS) (Kruskal and Wish 1978) on Bray–Curtis dissimilarity indices (Clarke and Green 1988) using r-package 'vegan' (Oksanen 2019). For this analysis, rare species, defined as species with less than two total occurrences, were excluded from the analysis to prevent them from appearing too influential in the graphical representation of the ordination (Poos and Jackson 2011). Differences between the treatments were tested with permutational multivariate analysis of variance (PERMANOVA, 999 permutations), incorporating experimental blocks as a random intercept. To test for the effect of predator exclusion on abiotic parameters, we used linear mixed-effect models (LMM) with 'block' as a random factor. Post hoc comparisons were used to test for significant differences between the effect of predator exclosure, open exclosure and control (r-package 'emmeans'; Lenth 2019).

Results

Benthic Ray Sediment Bioturbation

To examine benthic bioturbation rates, we surveyed newly formed ray pit and volumes on two consecutive days at the tidal flat Napus. The distribution of ray pits varied between 0 and 2 newly formed ray pits m^{-2}. The distribution of these pits related to the environmental predictors (distance to creek, distance to mangroves and elevation) was best described according concentrated foraging patterns (negative binomial distribution) versus random distribution (normal distribution; Appendix S1a). To estimate the surface that was bioturbated by the excavation of these pits, we used the average pit volume of 1475.87 cm^3 (n = 440 at Napus 2019) to calculate the bioturbation rates based on the number of newly formed ray pits on one single 24-h period in February 2021. To estimate the surface that was bioturbated by the excavation of these pits, we used the average pit volume of 1475.87 cm^3 (n = 440 at Napus 2019) to calculate the bioturbation rates based on the number of newly formed ray pits over one single 24-h period in February 2021. We found that ray pit excavation bioturbated the sediment surface with 3.7 ± 0.4% per day (mean ± SE) and up to 14.3% per day. This equals a volume of on average 765.3 ± 73.0 cm^{3}m^{-2} day^{-1} measured over one single 24-h period and is equivalent to a turnover rate of 27 days. The total surface covered with ray

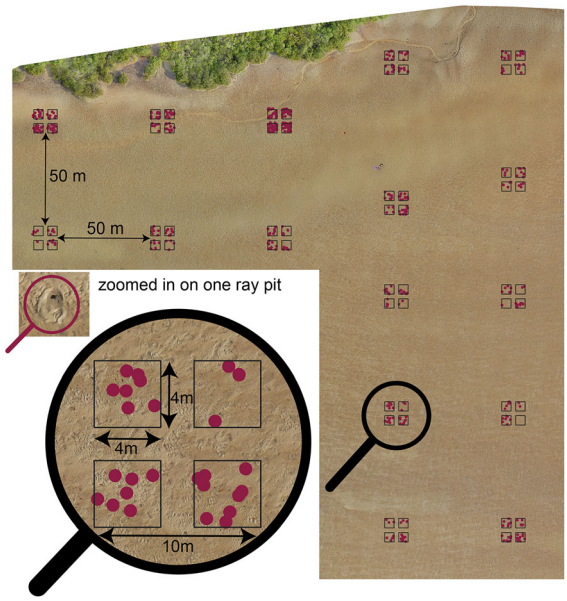

Figure 3. Annotations of new ray pits on the tidal flat Napus on February 16, 2021. An example of one zoomed in ray pit is shown in the top-left corner. High bioturbation of 3.70 ± 0.35% of the surface area per day was observed measured over one single 24-h period (mean ± SE). This bioturbation comes with a volume of 765.31 ± 72.97 cm^3 m^{-2} day^{-1} (mean ± SE).

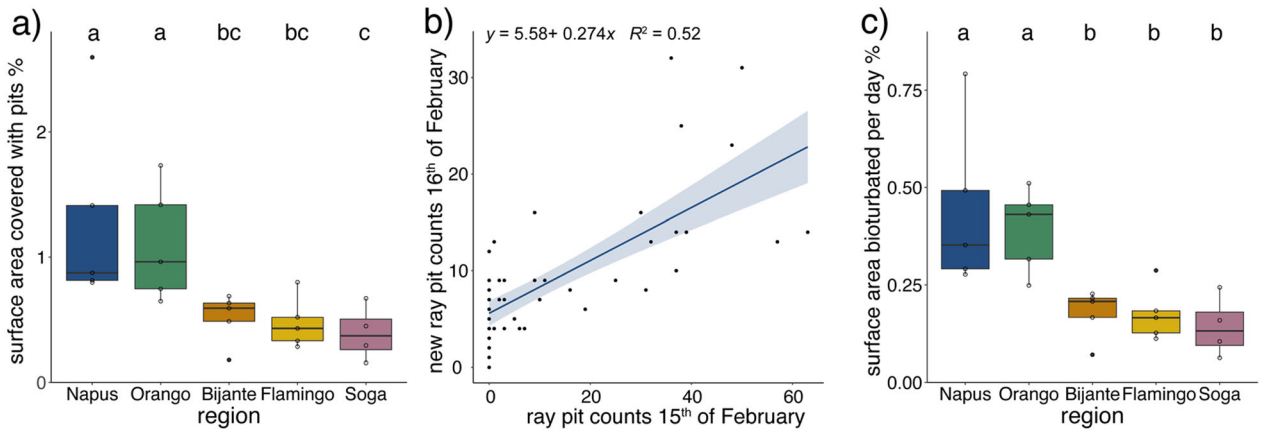

Figure 4. **a** High tidal flat surface area covered with ray pits in percentage, based on the observational survey with transects (n = 5 per tidal flat, Soga n = 4) in November 2019. Letters indicate significant differences tested with Tukey's post hoc; **b** relation between of the ray pit counts on February 15, 2021, and newly formed pit counts of February 16, 2021. The surface of the tidal flats bioturbated per day was calculated using linear regression and the ray pit abundances of Figure 3, resulting in **c** total surface area percentage bioturbated per day per tidal flat in November 2019 (n = 5 per tidal flat, Soga n = 4).

pits on the tidal flats of Napus on February 15 was 4.97 ± 0.68% (mean ± SE; Figure 3).

Consequently, we used the relationship between the total amount of pits and newly formed pits measured in 2021 to estimate the bioturbation rates on all five tidal flats measured in 2019. The relation between the total amount of ray pits on February 15 compared to the newly formed pits of February 16 could be described according a linear regression: $y = 5.58 + 0.274x$ (Figure 4b, $R^2 = 0.52$). Implementation of this linear regression on the measurements of November 2019 (start of the experiment, described in section below) implied that bioturbation rates at that particular moment ranged between 0.14 ± 0.04 and 0.44 ± 0.10% (mean ± SE, Figure 4c, 1-way ANOVA, $F_{4,19} = 7.1314$, $p < 0.001$). These bioturbation rates in February 2021 were 8.4 times higher at Napus compared to November 2019, and therefore, it is likely that bioturbation rates vary daily, seasonally and/or yearly.

Benthic Ray Pit Abundance, Spatial Distribution and Longevity

To test if the abundance of ray pits could be influenced by the tidal flat morphology; for example, ray pits erode faster under highly hydrodynamic conditions (O'Shea and others 2012), we counted the number of ray pits at five tidal flats through a field survey in November 2019. We found that the total excavated surface area significantly differed among tidal flats and ranged between 0.39 ± 0.50 and 1.30 ± 1.64% of the total tidal flat surface area (mean ± SE) (Figure 4a, one-way ANOVA, $F_{2,19} = 5.566$, $p = < 0.001$). In addition, there was a great level of ray pit spatial heterogeneity within the tidal flats. To explain the spatial distribution of ray pits within the tidal flat landscape, we investigated the relation of pit abundance to environmental parameters (Table 1). The distribution of these ray pits could be predicted (deviance explained 35.3%) based on sediment characteristics: median grain size D50, silt%, organic matter content, distance to the subtidal and emergence time (Table 1).

To test for a relationship between ray pit abundance and morphology, we measured the longevity of hand-made ray pits at two locations with differing exposure, but with comparable elevation (on average + 8.9 cm at the mangrove edge compared to exposed location). We found a 3.5 times faster pit volume decay rate at the exposed location with a coefficient of − 2.87 ($R^2 = 0.88$), compared to − 0.81 ($R^2 = 0.46$) at a location sheltered by the tidal flat itself (mangrove edge; Appendix S3). This means that, after 24 h, only 17.2% of ray pit volume remained in exposed areas, in contrast to 74.0% of the original pit volume remaining in sheltered areas.

Predator Exclusion Effects on Sediments and Macrozoobenthos

The exclusion of predators such as rays and shore birds created muddier and more stabilized sedi-

Table 1. Significance of Smoothers and Model Summary Statistics of Four Best Model Subsets Ranked by Lowest AICs of the GAM Predicting Ray Pit Abundance

Rank	Distance subtidal	Emergence time	Sediment OM	Region as random effect	Silt%	Grainsize (D50)	Distance gully	df	AICc	Weight	Deviance explained
1	+	+	+		+	+		30	2071.1	0.298	35.3
2	+	+	+	+	+	+		30	2071.1	0.297	35.1
4	+	+	+	+	+	+	+	37	2071.9	0.203	35.8
5	+	+	+		+	+	+	37	2071.9	0.203	35.9

The predictors are distance to subtidal water, emergence time, sediment median grainsize D50 in µm, sediment silt%, sediment organic matter content (OM) and region of the tidal flats as random effect. Environmental parameter included in the model is signified by the + symbol. So, empty cells indicate that the specific parameter is not included in that model. The ray pit abundance data include all five intertidal flats with intertidal flat as random factor.

ments, and a higher abundance of Capitellidae worms and greater biomass of Malacostraca over time (15 months). Silt and organic matter content were 20% (Tukey, $p < 0.01$) and 10% (Tukey, $p < 0.001$) higher, respectively, in the top-5 sediment layer of the exclosures than in the control plots in February 2021 (Table 2), while there were no differences in sediment properties at the start of the experiment (November 2019, Appendix S2). In addition, the exclosures showed − 17% sedimentation (Tukey, $p < 0.01$) and − 43% erosion (Tukey, $p < 0.0001$) after 15 months (Table 2), indicating higher sediment stability. Furthermore, we found no effects of the open exclosures on sediment properties (for example, median grain size, silt%, organic matter content, erosion, accretion) as the open exclosures yielded results similar to the controls (Table 2). We can therefore safely assume that the effects of the exclosures on sediment properties are the result of predator exclusion and not an effect of the exclosure structures themselves. Moreover, predator exclusion altered the macrozoobenthic community composition (after 15 months), based on species biomass (Figure 5, PERMANOVA, $n = 999$, $F = 6.38$, $p < 0.001$) and species abundance (Appendix S4: PERMANOVA, $n = 999$, abundance: $F = 3.52$, $p < 0.01$). In February 2021, this difference could partly be explained by 1.8 times higher abundance of polychaete worms of the Capitellidae family and a 4.0 times higher biomass of Malacostraca in the exclosure compared to control, while a 0.6 times lower abundance of both Pilargidae and Nereididae was observed (Appendix S5.1 and S5.2). The biomass of the bivalves *Tagelus adansonii* and *Senilia senilis* in the exclosure is responsible for outliers at both the start (three times higher compared to control in November 2019) and end (25 times higher compared to control in February 2021) (Appendix S5.1 and S5.2). At the start of the experiment, the macrozoobenthic communities did not differ between the exclosure and control for both species' biomass and abundance (Appendix S4.2 and S4.3, PERMANOVA, $n = 999$, abundance: $F = 0.53$, $p = 0.809$, biomass: $F = 0.76$, $p = 0.674$).

Discussion

Rays are sensitive to overfishing and are now rapidly disappearing from tidal flat ecosystems (Dulvy and others 2021). Rays can play an important role in determining tidal flats' community structure and morphology as natural physical disturbance by bioturbating the sediment. Bioturbation is considered a key factor in sediment transport, porosity and permeability (Thistle 1981; Thrush and others

Table 2. The Effects of Predator Exclosure on Sediment Properties, Accretion and Erosion Levels Compared to the Open Exclosure and Control Treatments

Sediment layer	Variable	Unit	Predator exclosure Mean (SE)	Open exclosure Mean (SE)	Control Mean (SE)
Top 1 cm	Median grain size (D50)	µm	217.87^{a} (1.93)	223.12^{ab} (4.40)	231.93^{b} (4.69)
Top 1 cm	Silt < 63 µm	%	3.81^{a} (0.19)	3.25^{b} (0.20)	2.81^{b} (0.17)
Top 1 cm	Organic matter (loss of ignition)	%	1.01^{a} (0.02)	0.95^{ab} (0.03)	0.90^{b} (0.03)
Top 5 cm	Median grain size (D50)	µm	221.43^{a} (3.18)	221.14^{a} (4.62)	232.86^{a} (3.91)
Top 5 cm	Silt < 63 µm	%	2.97^{a} (0.10)	2.70^{ab} (0.13)	2.45^{b} (0.13)
Top 5 cm	Organic matter (loss of ignition)	%	0.88 (0.02)	0.81 (0.02)	0.80 (0.03)
na	Ray pits	Fraction	0.00 (0.00)	0.48 (0.06)	0.33 (0.06)
na	Accretion	Cm	5.74^{a} (0.28)	6.39^{ab} (0.25)	6.72^{b} (0.23)
na	Erosion	Cm	4.72^{a} (0.32)	6.35^{b} (0.35)	6.75^{b} (0.26)
na	Net surface change	Cm	1.03^{a} (0.32)	0.04^{a} (0.44)	− 0.02^{a} (0.38)

Letters indicate significant differences tested with Tukey's post hoc.

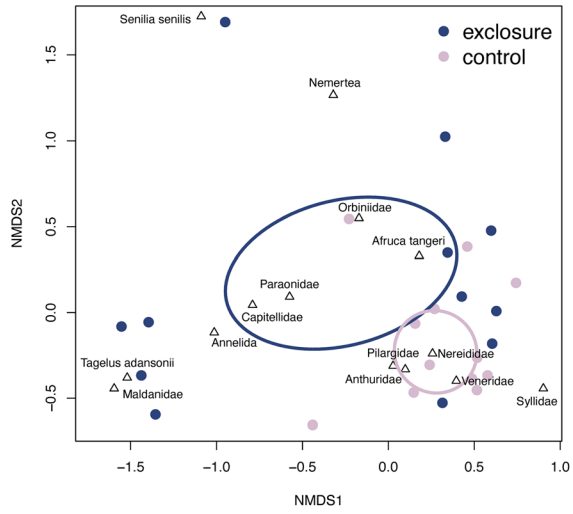

Figure 5. Ordination of taxa composition based on species biomass (ash free dry weight m^{-2}) in the predator exclosures compared to the control plots without any exclusion visualized with Non-Metric Multidimensional Scaling (nMDS) on Bray–Curtis dissimilarity indices and reliable ordination (stress value < 0.2). Ellipses indicate the precision of estimated centroid (se) with 95% confidence interval.

1991; Meysman and others 2006). In addition, however, the ecological role of these foundation species in tidal ecosystems is still relatively poorly understood. We therefore linked ray bioturbation—and the absence of this behavior—to landscape-scale tidal flat geomorphology in a relatively less-exploited (that is, high abundance of benthic rays) tropical tidal system (Leurs and others 2023b). These ray abundances are estimated based on small-scale fisheries ray catches by Leurs and others (unpublished) using satellite-based vessel counts and a short-term observer program that estimated that 896–2685 rays were captured daily in 2020 in the Bijagós Archipelago (Leur and others unpublished). We found that benthic rays affect tidal flat sediment dynamics by digging excavations and bioturbating of 3.7% of the total sediment surface per day over one single 24-h period. This implies that the entire sediment surface area is reworked by rays every 27 days. These bioturbation rates varied substantially on a landscape level, among years, tidal flats and within one tidal flat landscape. Furthermore, the absence of natural physical disturbance by rays, simulated by a long-term exclosure experiment, increased sediment stability (reduced erosion and accretion) and increased silt% and organic matter content in the top sediment layer. This indicates the importance of natural physical disturbance by benthic rays on tidal flat biogeomorphology. In addition, the long-term (15 months) exclosure experiment changed the macrozoobenthos community composition by a higher abundance of Capitellidae worms and greater biomass of Malacostraca over time. Although we were unable to separately exclude rays or wading birds in the predator exclosure experiment, we can safely assume that the bioturbation effects are due to ray excavation because birds feed without bioturbating the sediment surface (Lourenço and others 2017, 2018). Furthermore, previous research found that bioturbation by benthic rays can change the sediment biogeochemistry of sandflats by rapid remineralization of organic matter, slowed flushing near the ray pits and increased reactive carbon supply (D'Andrea and others 2002). Hence, overexploitation of benthic rays may alter ecosystem functioning of threatened tidal flat seascapes.

Benthic rays can substantially alter tidal flat sediment turnover by sediment bioturbation and the magnitude of sediment displacement rates (mean of 765.31 cm^3m^{-2} day^{-1}) found in this study further underlines the importance of these ray-induced processes for tidal flat morphology. The sediment bioturbation rates that we found (on average 3.7% and a maximum of 14.3% day^{-1} over one single 24-h period) were higher than the previously reported stingray bioturbation rates, for example, 2.42% in 7 days in Ningaloo reef in Australia (Grant 1983; Sherman and others 1983; O'Shea and others 2012) or 1.4% day^{-1} on intertidal sandflats of the North Island of New Zealand (Thrush and others 1991). Our sediment displacement rates fall within the range of previous reported studies (Lynn-Myrick and Flessa 1996; O'Shea and others 2012). However, where previous research elaborates that benthic ray bioturbation has most relevance at the micro- and meso-scales (O'Shea and others 2012) or studied at smaller tidal areas (0.11 km^2 and only one tidal flat (Takeuchi and Tamaki 2014), we demonstrated that ray bioturbation plays a significant role on a landscape scale throughout the region (study area of 0.5–0.75 km^2 per tidal flat * five tidal flats). This is comparable to the landscape scale at which flamingos and fiddler crabs together create essential microhabitats in Mauritanian tidal flats (El-Hacen and others 2019). Bioturbation rates may vary across studies because of differences in local ray densities, species-specific bioturbating behavior and body size or the visibility of the pit on the tidal flat surface (Flowers and others 2021).

Benthic ray bioturbation rates are influenced by the ray densities (biotic) and pit longevity (abiotic). First, ray densities are affected by the season or year (Leurs and others 2023b). Leurs and others (2023b) found that seasonal differences in species richness and species composition of elasmobranch are caused by changes in stingray (the pearl whipray *Fontitrygon margaritella)* abundances, and that species composition differed between non-protected and protected areas when seasonality is taken into account. In addition, we found an 8.4 × higher bioturbation rates in February 2021 compared to November 2019 and (Thrush and others 1991) observed more prevalence of rays during summer (November to March in New Zealand). Likewise, industrial fishing activities show highest mean catches of benthic rays in April–June along the coast of Guinee-Bissau (Leurs and others 2021). Second, ray densities can vary among tidal flats within the region, for example, bioturbation rate ranging from 0.2 to 14.3% per day in our study. Third, ray spatial distribution can differ within the tidal flat landscape because of spatial heterogeneity such as food availability (Hines and others 1997; Ajemian and Powers 2012), predator risk (Strong and others 1990; Stephens and others 2007) and the risk of entrapment in areas that will fall dry with the receding tides (Brinton and Curran 2017; Leurs and others 2023a). On the other hand, we found that exposure to hydrodynamic forces of the tidal flat played an important role in the longevity of the ray pits (abiotic) as a result of more exposure to hydrodynamic forces and less cohesive soil (Wang and others 2019). Our study showed that only 17.2% of pit volume was left after 24 h on exposed areas compared to 74.0% on an area sheltered by the tidal flat; thus, a shorter longevity (< 1 day) of ray pits in high exposed areas might give an underestimation of benthic ray bioturbation. In summary, the interplay of biotic and abiotic factors determines the measured tidal flats' bioturbation rates by benthic rays and, in addition to bioturbation, benthic rays further impact the environment by foraging on macrozoobenthos (Lynn-Myrick and Flessa 1996; O'Shea and others 2013; Lim and others 2019).

We found that predator exclusion significantly changed the macrozoobenthic community, specifically higher Capitellidae abundances and malacostraca biomass. However, these results should be interpreted with caution since we were not able to exclude rays only, but also excluded shore birds. Previous research observed no impact and suggested ineffective ray exclusion (O'Shea 2012) or used a limited number ($n = 2$) of replicates and reported scouring (VanBlaricom 1982). In addition, Thrush and others (1994) found a lower number of bivalve recruits in predator (ray + bird) exclosure, but were also unable to distinguish ray and bird effects due to seasonality. In the Bijagós, the most abundant meso-predatory ray, *F. margaritella*, shows a generalist's diet with relative contributions of 30–35% by crustaceans and 17–25% by polychaetes (Clements and others 2022). These dietary preferences match the observed community changes in the exclosure experiment. Overall, a ray's turbulent foraging strategy may especially affect long-lived, sedentary species (O'Shea 2012; Jacobsen and Bennett 2013; Freitas and others 2019). Because the standing macrozoobenthic biomass in the Bijagós Archipelago is on average low compared to other tidal flat ecosystems (Lourenço and others 2018; Meijer and others 2021), it is likely that the observed high ray pit abundances (up to a mean of 1.30% per total surface area), combined with low macrozoobenthic

biomass, indicate a high foraging pressure by benthic rays and other (meso-)predators such as shorebirds. Shorebirds are predators with small trophic niches that feed without bioturbating the mudflat (Catry and others 2016; Lourenço and others 2017, 2018). Shorebirds in the Bijagós Archipelago forage on fiddler crabs, polychaetes (*Nereis*, *Glycera* and *Marphysa*) and the bivalve *Dosinia isocardia* (Lourenço and others 2017), but consume in general a high diversity of prey (Correia and others 2023). In general, shorebirds are major players in intertidal food webs because to occupy a central niche (Mathot and others 2018) and recent findings suggest that (meso-)predators such as sharks and rays (that is, high-tide predators in the intertidal) occupy a similar central niche as shore birds in intertidal food webs and should therefore be considered in intertidal ecology (Leurs and others 2023a). High foraging pressure of rays may even cause a food conflict with shorebirds foraging on the same tidal flats and competing for the same scarce prey species (Lourenço and others 2017, 2018) and affect tidal, subtidal and terrestrial food webs through shorebird migration along the East Atlantic Flyway.

The importance of ray bioturbation to the ecosystem depends on the magnitude of other environmental and biotic factors that can disturb the sediment such as tidal waves and currents, extreme weather events and the impact of other bioturbating organisms. High forces of water movement can displace large volumes of sediments that may overrule the impact of ray bioturbation. For example, D'Andrea and others (2002) described that ray pits are short-term depositional center for reactive organic matter that alter the sediment structure for 1–4 days. This study is limited by the amount of information that we collected regarding sediment displacement rates of tidal flats controlled by water movement. It is known, however, that the Bijagós Archipelago is a relatively stable intertidal ecosystem with low changes in tidal flat area compared to other intertidal areas of the world (Murray and others 2019, 2022). In addition, West Africa is relatively low in extreme weather events such as cyclones because most Atlantic tropical cyclones are developed in the West African region moving from east to west (Goldenberg and Shapiro 1996; Hopsch and others 2007). Moreover, we observed low presence of burrows from other bioturbation species such as calianassid shrimps (Callianassidae) that can overturn sediments at an estimated peak rate of 0.47–0.56 m^{-3} m^{-2} $year^{-1}$ (Suchanek and Colin 1986; Myrick and Flessa 2017). Although this study has its limitations, our results show that short-term ray bioturbation effects on the sediment are maintained at a landscape scale and may co-shape tidal flat morphology along with abiotic settings.

Our study showed that complex biogeomorphic interactions, in which organisms influence sedimentary processes, underpin tidal flats ecosystem functioning. The protection of bioturbating species should be better integrated in coastal management plans for tidal flat conservation because the natural physical disturbance by rays plays an important role in sediment turnover rates and structuring of the macrozoobenthic community on landscape scales. Since tidal flats are highly connected ecosystems globally, the need for protection, both locally and internationally on a highly interconnected habitat level is further emphasized. For example, fishing activities in adjacent marine habitats affect the ray population in tidal ecosystems and tidal ecosystems (Dulvy and others 2021; Leurs and others 2021). Hence, disruption of tidal flats' high ecological value can have consequences for other connected ecosystems and vice versa.

Conclusion

We conclude that benthic rays affect landscape-scale sediment processes and community structure by bioturbation, and thus tidal flat biogeomorphology. This study highlights that local ecological processes (ray bioturbation) play a significant role at the landscape scale. Neither marine nor terrestrial protected areas are developed to prioritize tidal flat conservation and tidal flat conservation generally focuses on total coverage instead of targeting valuable ecosystem services or species (Dhanjal-Adams and others 2016; Hill and others 2021). Therefore, coastal management strategies to protect intertidal ecosystems may benefit from an integral and connective approach linking the subtidal offshore (industrial) fishing activities to intertidal ecosystem functioning. Changes in species abundance as a result of these offshore fishing activities target on highly mobile species, such as benthic rays that migrate in both subtidal and intertidal waters, can affect sedimentary processes in the intertidal with associated consequences for species composition, for example, dominance of species due to reduced physical disturbance.

Acknowledgements

Many thanks go to L. Dos Santos, S. João Correia, Luta, Quintino, O. Clements T. Zuidewind for field assistance. We would like to thank IBAP for being a

partner and providing logistical support. In addition, thanks to NGO Tiniguena-Esta Terra É Nossa, Management authorities of the Urok and Orango National Parks, MAVA foundation and local communities for providing access to their lands. Our thanks go to A. Coelho, M. Henriques, L. Kleine Schaars, M. Laveleye and L. Niemeijer for providing identification keys to the macrozoobenthos. We would like to thank M. Zwarts and J. Heusinkveld from the Fieldwork Company for drone and logistic assistance. This study was funded by the MAVA Foundation (Waders of the Bijagós) and LG by the Dutch Research Council (NWO016.VENI.181.087). Appropriate ethics, permits and other approvals were obtained for the research included in this manuscript.

DATA AVAILABILITY

Data are available via the DataverseNL repository at https://doi.org/10.34894/QIWNHC.

Declarations

Conflict of interest

The authors declare no conflict of interest.

OPEN ACCESS

REFERENCES

Ajemian MJ, Powers SP. 2012. Habitat-specific feeding by cownose rays (*Rhinoptera bonasus*) of the northern Gulf of Mexico. Environ Biol Fishes 95:79–97.

Alongi DM. 2014. Carbon cycling and storage in mangrove forests. Ann Rev Mar Sci 6:195–219.

Alongi DM. 2018. Blue carbon, 1st edn. Cham, Switzerland: Springer International Publishing.

Bartón K. 2022. Package ''MuMIn'' title multi-model inference.

Bascompte J, Melián CJ, Sala E. 2005. Interaction strength combinations and the overfishing of a marine food web. Proc Natl Acad Sci U S A 102:5443–5447.

Baum JK, Myers RA. 2004. Shifting baselines and the decline of pelagic sharks in the Gulf of Mexico. Ecol Lett 7:135–145.

Baum JK, Myers RA, Kehler DG, Worm B, Harley SJ, Doherty PA. 2003. Collapse and conservation of shark populations in the Northwest Atlantic. Science 299:389–392.

Bird ECF. 2011. Coastal geomorphology: an introduction. Hoboken: Wiley.

Brinton CP, Curran MC. 2017. Tidal and diel movement patterns of the Atlantic stingray (*Dasyatis sabina*) along a stream-order gradient. Mar Freshw Res 68:1716.

Campredon P, Catry P. 2016. Bijagos archipelago (Guinea-Bissau). The Wetland book, . Springer, Netherlands: Dordrecht. pp 1–8.

Catry T, Lourenço PM, Lopes RJ, Carneiro C, Alves JA, Costa J, Rguibi-Idrissi H, Bearhop S, Piersma T, Granadeiro JP. 2016. Structure and functioning of intertidal food webs along an avian flyway: a comparative approach using stable isotopes. Funct Ecol 30:468–478.

Clarke KR, Green RH. 1988. Statistical design and analysis for a ''biological effects'' study. Mar Ecol Progr Ser 46:213–226.

Clements ON, Leurs G, Witbaard R, Pen I, Verkuil YI, Govers LL. 2022. Growth, maturity, and diet of the pearl whipray (*Fontitrygon margaritella*) from the Bijagós Archipelago Guinea-Bissau. PeerJ 10:e12894.

Cohen JE, Pimm SL, Yodzis P, Saldaña J. 1993. Body sizes of animal predators and animal prey in food webs. J Anim Ecol 62:67–78.

Compton TJ, Holthuijsen S, Koolhaas A, Dekinga A, ten Horn J, Smith J, Galama Y, Brugge M, van der Wal D, van der Meer J, van der Veer HW, Piersma T. 2013. Distinctly variable mudscapes: distribution gradients of intertidal macrofauna across the Dutch Wadden Sea. J Sea Res 82:103–116.

Correia E, Granadeiro JP, Santos B, Regalla A, Mata VA, Catry T. 2023. Trophic ecology of a migratory shorebird community at a globally important non-breeding site: combining DNA metabarcoding and conventional techniques. Mar Ecol Prog Ser 705:127–144.

D'Andrea AF, Aller RC, Lopez GR. 2002. Organic matter flux and reactivity on a South Carolina sandflat: the impacts of porewater advection and macrobiological structures. Limnol Oceanogr 47:1056–1070.

Dhanjal-Adams KLA, Hanson JO, Murray NJ, Phinn SR, Wingate CVR, Mustin K, Lee JR, Allan JR, Cappadonna JL, Studds CE, Clemens RS, Roelfsema CM, Fuller RA. 2016. The distribution and protection of intertidal habitats in Australia. Emu 116:208–214.

Diop M, Dossa J. 2011. 30 years of shark fishing in west africa 30 years of shark fishing in West Africa. Condé-sur-Noireau, France: FIBA.

Dulvy NK, Fowler SL, Musick JA, Cavanagh RD, Kyne PM, Harrison LR, Carlson JK, Davidson LN, Fordham SV, Francis MP, Pollock CM, Simpfendorfer CA, Burgess GH, Carpenter KE, Compagno LJ, Ebert DA, Gibson C, Heupel MR, Livingstone SR, Sanciangco JC, Stevens JD, Valenti S, White WT. 2014. Extinction risk and conservation of the world's sharks and rays. Elife 3:e00590.

Dulvy NK, Pacoureau N, Rigby CL, Pollom RA, Jabado RW, Ebert DA, Finucci B, Pollock CM, Cheok J, Derrick DH, Her-

man KB, Sherman CS, VanderWright WJ, Lawson JM, Walls RHL, Carlson JK, Charvet P, Bineesh KK, Fernando D, Ralph GM, Matsushiba JH, Hilton-Taylor C, Fordham SV, Simpfendorfer CA. 2021. Overfishing drives over one-third of all sharks and rays toward a global extinction crisis. Curr Biol 31:4773–4787.

El-Hacen EHM, Bouma TJ, Oomen P, Piersma T, Olff H. 2019. Large-scale ecosystem engineering by flamingos and fiddler crabs on West-African intertidal flats promote joint food availability. Oikos 128:753–764.

Ferretti F, Worm B, Britten GL, Heithaus MR, Lotze HK. 2010. Patterns and ecosystem consequences of shark declines in the ocean. Ecol Lett 13:1055–1071.

Flowers KI, Heithaus MR, Papastamatiou YP. 2021. Buried in the sand: uncovering the ecological roles and importance of rays. Fish Fish (oxf) 22:105–127.

Freitas RHA, Aguiar AA, Freitas AKCHA, Lima SMQ, Valentin JL. 2019. Unravelling the foraging behavior of the southern stingray, Hypanus americanus (Myliobatiformes: Dasyatidae) in a Southwestern Atlantic MPA. Neotrop Ichthyol 17. http://www.scielo.br/j/ni/a/fZ57Gygh6b5nLVxrBsQy3bS/abstract/?lang=en.

Goldenberg SB, Shapiro LJ. 1996. Physical mechanisms for the association of El Niño and West African rainfall with atlantic major hurricane activity. J Clim 9:1169–1187.

Granadeiro JP, Belo J, Henriques M, Catalão J, Catry T. 2021. Using sentinel-2 images to estimate topography, tidal-stage lags and exposure periods over large intertidal areas. Remote Sens 13:1–17.

Grant J. 1983. The relative magnitude of biological and physical sediment reworking in an intertidal community. J Mar Res 41:673–689.

Grubbs RD, Carlson JK, Romine JG, Curtis TH, McElroy WD, McCandless CT, Cotton CF, Musick JA. 2016. Critical assessment and ramifications of a purported marine trophic cascade. Sci Rep 6:20970.

Hartig F. 2023. DHARMa: residual diagnostics for hierarchical ## (Multi-Level / Mixed) regression models. http://florianhartig.github.io/DHARMa/.

Hill NK, Woodworth BK, Phinn SR, Murray NJ, Fuller RA. 2021. Global protected-area coverage and human pressure on tidal flats. Conserv Biol 35:933–943.

Hines AH, Whitlatch RB, Thrush SF, Hewitt JE, Cummings VJ, Dayton PK, Legendre P. 1997. Nonlinear foraging response of a large marine predator to benthic prey: eagle ray pits and bivalves in a New Zealand sandflat. J Exp Mar Bio Ecol 216:191–210.

Hopsch SB, Thorncroft CD, Hodges K, Aiyyer A. 2007. West African storm tracks and their relationship to atlantic tropical cyclones. J Clim 20:2468–2483.

Jacobsen IP, Bennett MB. 2013. A comparative analysis of feeding and trophic level ecology in stingrays (Rajiformes; Myliobatoidei) and electric rays (Rajiformes: Torpedinoidei). PLoS One 8:e71348.

Jennings S, Pinnegar JK, Polunin NVC, Boon TW. 2001. Weak cross-species relationships between body size and trophic level belie powerful size-based trophic structuring in fish communities. J Anim Ecol 70:934–944.

Kruskal J, Wish M. 1978. Multidimensional scaling. Thousand Oaks: SAGE Publications Inc.

Lenth R. 2019. emmeans: estimated marginal means, aka Least-Squares Means. R package version 461 1.4.3.01. https://CRAN-project.org/package=emmeans.

Leurs G, van der Reijden KJ, Cheikhna Lemrabott SY, Barry I, Nonque DM, Olff H, Ledo Pontes S, Regalla A, Govers LL. 2021. Industrial fishing near west african marine protected areas and its potential effects on mobile marine predators. Front Mar Sci 8:177. https://doi.org/10.3389/fmars.2021.602917.

Leurs G, Nieuwenhuis BO, Zuidewind TJ, Hijner N, Olff H, Govers LL. 2023. Where land meets sea: intertidal areas as key-habitats for sharks and rays. Fish Fish. https://doi.org/10.1111/faf.12735.

Leurs G, Verkuil YI, Hijner N, Saalmann F, Dos Santos L, Regalla A, Ledo Pontes S, Yang L, Naylor GJP, Olff H, Govers LL. 2023b. Addressing data-deficiency of threatened sharks and rays in a highly dynamic coastal ecosystem using environmental DNA. Ecol Indic 154:110795.

Lim KC, Chong VC, Lim P-E, Yurimoto T, Loh KH. 2019. Feeding ecology of three sympatric species of stingrays on a tropical mudflat. J Mar Biol Assoc U K 99:999–1007.

Lourenço PM, Granadeiro JP, Catry T. 2018. Low macroinvertebrate biomass suggests limited food availability for shorebird communities in intertidal areas of the Bijagós archipelago (Guinea-Bissau). Hydrobiologia 816:197–212.

Lourenço PM, Catry T, Granadeiro JP. 2017. Diet and feeding ecology of the wintering shorebird assemblage in the Bijagós archipelago, Guinea-Bissau. J Sea Res. https://www.sciencedirect.com/science/article/pii/S1385110116303616.

Lynn-Myrick J, Flessa KW. 1996. Bioturbation rates in Bahía La Choya, Sonora, Mexico. Cienc Mar 22:23–46.

Mathot KJ, Piersma T, Elner RW. 2018. Shorebirds as integrators and indicators of mudflat ecology. In: Beninger PG, Ed. Mudflat ecology, . Cham: Springer International Publishing. pp 309–338.

Meijer KJ, El-Hacen E-HM, Govers LL, Lavaleye M, Piersma T, Olff H. 2021. Mangrove-mudflat connectivity shapes benthic communities in a tropical intertidal system. Ecol Indic 130:108030.

Meysman FJR, Middelburg JJ, Heip CHR. 2006. Bioturbation: a fresh look at Darwin's last idea. Trends Ecol Evol 21:688–695.

Murray NJ, Phinn SR, DeWitt M, Ferrari R, Johnston R, Lyons MB, Clinton N, Thau D, Fuller RA. 2019. The global distribution and trajectory of tidal flats. Nature 565:222–225.

Murray NJ, Worthington TA, Bunting P, Duce S, Hagger V, Lovelock CE, Lucas R, Saunders MI, Sheaves M, Spalding M, Waltham NJ, Lyons MB. 2022. High-resolution mapping of losses and gains of Earth's tidal wetlands. Science 376:744–749.

Myers RA, Baum JK, Shepherd TD, Powers SP, Peterson CH. 2007. Cascading effects of the loss of apex predatory sharks from a coastal ocean. Science 315:1846–1850.

Myrick JL, Flessa KW. 2017. Bioturbation rates in Bahía La Choya, Sonora, Mexico. Cienc Mar 22:23–46.

Needham HR, Pilditch CA, Lohrer AM, Thrush SF. 2011. Context-specific bioturbation mediates changes to ecosystem functioning. Ecosystems 14:1096–1109.

Nolte S, Koppenaal EC, Esselink P, Dijkema KS, Schuerch M, De Groot AV, Bakker JP, Temmerman S. 2013. Measuring sedimentation in tidal marshes: A review on methods and their applicability in biogeomorphological studies.

O'Shea OR, Thums M, Van Keulen M, Meekan M. 2012. Bioturbation by stingrays at Ningaloo Reef, Western Australia. Mar Freshwater Res 63:189–197.

O'Shea OR, Thums M, van Keulen M, Kempster RM, Meekan MG. 2013. Dietary partitioning by five sympatric species of stingray (Dasyatidae) on coral reefs. J Fish Biol 82:1805–1820.

O'Shea OR. 2012. The Ecology and Biology of Stingrays (Dasyatidae) at Ningaloo Reef, Western Australia. p. 214.

Oksanen J. 2019. Vegan: ecological diversity.

QGIS Development Team AE, Others. 2018. QGIS geographic information system. Open source geospatial foundation project.

Pauly D. 1998. Fishing down marine food webs. Science 279(5352):860–863.

Pinnegar JK, Polunin NVC, Francour P, Badalamenti F, Chemello R, Harmelin-Vivien M-L, Hereu B, Milazzo M, Zabala M, D'anna G, Pipitone C. 2000. Trophic cascades in benthic marine ecosystems: lessons for fisheries and protected-area management. Environ Conserv 27:179–200.

Poos MS, Jackson DA. 2011. Addressing the removal of rare species in multivariate bioassessments: the impact of methodological choices. Ecol Indic 18:82–90.

R Core Team. 2017. R: a language and environment for statistical computing. https://www.R-project.org/.

Ramsar Convention Secretariat. 2014. Ramsar Sites Information Service. https://rsis.ramsar.org/ris/2198.

Salvig JC, Asbirk S, Kjeldsen JP, Rasmussen PAF. 1994. Wintering waders in the Bijagos Archipelago Guinea-Bissau 1992–1993. Ardea 82:137–142.

Sherman KM, Reidenauer JA, Thistle D, Meeter D. 1983. Role of a natural disturbance in an assemblage of marine free-living nematodes. Mar Ecol Prog Ser 11:23–30.

Sherman CS, Heupel MR, Moore SK, Chin A, Simpfendorfer CA. 2020. When sharks are away, rays will play: effects of top predator removal in coral reef ecosystems. Mar Ecol Prog Ser 641:145–157.

Sherman CS, Simpfendorfer CA, Pacoureau N, Matsushiba JH, Yan HF, Walls RHL, Rigby CL, VanderWright WJ, Jabado RW, Pollom RA, Carlson JK, Charvet P, Bin Ali A, Fahmi Cheok J, Derrick DH, Herman KB, Finucci B, Eddy TD, Palomares MLD, Avalos-Castillo CG, Kinattumkara B, Blanco-Parra M-D-P, Dharmadi EM, Fernando D, Haque AB, Mejía-Falla PA, Navia AF, Pérez-Jiménez JC, Utzurrum J, Yuneni RR, Dulvy NK. 2023. Half a century of rising extinction risk of coral reef sharks and rays. Nat Commun 14:15.

Smith JW, Merriner JV. 1985. Food habits and feeding behavior of the cownose ray, *Rhinoptera bonasus*, in lower Chesapeake Bay. Estuaries 8:305–310.

Stephens DW, Brown JS, Ydenberg RC, Eds. 2007. Foraging. Chicago, IL: University of Chicago Press.

Stevens JD, Bonfil R, Dulvy NK, Walker PA. 2000. The effects of fishing on sharks, rays, and chimaeras (chondrichthyans), and the implications for marine ecosystems. ICES J Mar Sci 57:476–494.

Strong WR, Snelson FF, Gruber SH. 1990. Hammerhead shark predation on stingrays: an observation of prey handling by Sphyrna mokarran. Copeia 1990(3):836–840.

Suchanek TH, Colin PL. 1986. Rates and effects of bioturbation by invertebrates and fishes at Enewetak and Bikini Atolls. Bull Mar Sci 38:25–34.

Takeuchi S, Tamaki A. 2014. Assessment of benthic disturbance associated with stingray foraging for ghost shrimp by aerial survey over an intertidal sandflat. Cont Shelf Res 84:139–157.

Temmerman S, Meire P, Bouma TJ, Herman PMJ, Ysebaert T, De Vriend HJ. 2013. Ecosystem-based coastal defence in the face of global change. Nature 504:79–83.

Thistle D. 1981. Natural physical disturbances and communities of marine soft bottoms. Mar Ecol Prog Ser 6:223–228.

Thrush SF, Pridmore RD, Hewitt JE, Cummings VJ. 1991. Impact of ray feeding disturbances on sandflat macrobenthos: Do communities dominated by polychaetes or shellfish respond differently? Mar Ecol Prog Ser 69:245–252.

Thrush SF, Pridmore RD, Hewitt JE, Cummings VJ. 1994. The importance of predators on a sandflat: interplay between seasonal changes in prey densities and predator effects. Mar Ecol Prog Ser 107:211–222.

van de Koppel J, van der Heide T, Altieri AH, Eriksson BK, Bouma TJ, Olff H, Silliman BR. 2015. Long-distance interactions regulate the structure and resilience of coastal ecosystems. Ann Rev Mar Sci 7:139–158.

van der Zee EM, Angelini C, Govers LL, Christianen MJA, Altieri AH, van der Reijden KJ, Silliman BR, van de Koppel J, van der Geest M, van Gils JA, van der Veer HW, Piersma T, de Ruiter PC, Olff H, van der Heide T. 2016. How habitat-modifying organisms structure the food web of two coastal ecosystems. Proc R Soc B Biol Sci 283:20152326. https://doi.org/10.1098/rspb.2015.2326.

Van Roomen M, Schekkerman H, Delany S, Van Winden E, Flink S, Langendoen T, Nagy S. 2011. Overview of monitoring work on numbers, reproduction and survival of waterbird populations important in the Wadden Sea and the East Atlantic Flyway. Nijmegen: SOVON.

VanBlaricom GR. 1982. Experimental analyses of structural regulation in a marine sand community exposed to oceanic swell. Ecol Monogr 52:283–305.

Wang Y, Wang YP, Yu Q, Du Z, Wang ZB, Gao S. 2019. Sand-mud tidal flat morphodynamics influenced by alongshore tidal currents. J Geophys Res Oceans 124:3818–3836.

Winemiller KO, Rose KA. 1992. Patterns of life-history diversification in North American fishes: implications for population regulation. Can J Fish Aquat Sci 49:2196–2218.

Wood SN. 2017. Generalized additive models. Chapman and Hall/CRC. https://doi.org/10.1201/9781315370279